

# Study of Phase Stability in NiPt Systems

Durga Paudyal, Tanusri Saha-Dasgupta and Abhijit Mookerjee

S.N. Bose National Centre for Basic Sciences, JD Block, Sector 3, Salt Lake City,  
Kolkata 700098, India

email: dpaudyal@bose.res.in, tanusri@bose.res.in, abhijit@bose.res.in

**Abstract.** We have studied the problem of phase stability in NiPt alloy system. We have used the augmented space recursion based on the TB-LMTO as the method for studying the electronic structure of the alloys. In particular, we have used the relativistic generalization of our earlier technique. We note that, in order to predict the proper ground state structures and energetics, in addition to relativistic effects, we have to take into account charge transfer effects with precision.

PACS numbers: 71.20,71.20c

## 1. Introduction.

There has been growing interest in the study of alloy phase ordering and segregation using first principles techniques. In order to study these phenomena one needs a derivation of the configurational energy for the alloy system. Different models have been proposed in which the configurational energies are expressed in terms of effective multi-site interactions, in particular effective pair interactions [1]. The analysis of alloy ordering tendencies and phase stability reduces to the accurate and reliable determination of effective pair interactions. There are two different approaches of obtaining the effective pair interactions. One approach is to start with electronic structure calculations of the total energy of ordered super-structures of the alloy and to invert these total energies to obtain the effective pair interactions. This is the Connolly-Williams method [2]. The other approach is to start from the completely disordered phase, set up a perturbation in the form of concentration fluctuations associated with an ordered phase and study whether the alloy can sustain such a perturbation. This includes approaches like the generalized perturbation method (GPM)[3], the embedded cluster method (ECM)[4]. Most of the works on the electronic structure of the disordered alloys have been based so far on the coherent potential approximation (CPA). The CPA being a single-site approximation cannot take into account the effect at a site of its immediate environment. In an attempt to go beyond the single site approximation, de Fontaine and his group followed a different approach of direct configurational averaging (DCA) [5], without resorting to any kind of single-site approximation. The effective pair and multi-site interactions were calculated directly in real space for given

configurations and the averaging was done in a brute force way by summing over different configurations. Invariably, the number of configurations was finite and convergence of the results with increasing number of configurations is yet to be available.

Saha *et al* [6] have introduced the augmented space recursion (ASR) based on the augmented space formalism (ASF) first suggested by Mookerjee [7] coupled with the recursion method of Haydock *et al* [8]. Within ASF the configuration averaging is carried out without having to resort to any single-site approximation. The recursion method allows us to take into account the effect of the environment of a given site. Moreover, the convergence of various physical quantities calculated through recursion with the number of recursion steps and subsequent termination has been studied in great detail [9]. Among advantages of the ASR in going beyond the single-site approximation is the possibility of inclusion of local lattice distortions which is important in the case of alloys with large size mismatch between components as in the case of NiPt. In an earlier paper Saha and Mookerjee [10] had discussed the effect of local lattice distortion on the electronic structures of CuPd and CuBe alloys using the ASR. This allows the structure matrices to randomly take values  $S_{RR'}^{AA}$ ,  $S_{RR'}^{AB}$ ,  $S_{RR'}^{BA}$  or  $S_{RR'}^{BB}$ , depending on the occupation of the sites  $R$  and  $R'$ . The augmented space recursion coupled with orbital peeling technique [11] to evaluate small energy differences associated with band structure energies has been successfully used in past to describe the phase formation in alloys [12].

In the present communication we focus on the application of this method for phase stability study in NiPt alloys. This system of alloys is of importance because of the possible need for relativistic corrections due to the heavy mass of Pt as well as effects due to charge transfer and size mismatch between Ni and Pt. This therefore forms a perfect candidate for testing the applicability and limitations of our formalism, bringing in the relative importance of various effects for the accurate description of the system. The previous studies of ordered and substitutionally disordered NiPt alloy systems have shown the importance of inclusion of relativistic effects. Treglia and Ducastelle [13] had shown that late transition metal alloys should exhibit phase separating tendencies but they argue that the exceptional ordering behavior of NiPt is due to the relativistic corrections. In a first principle study, Pinski *et al* [14] found that the disordered fcc  $\text{Ni}_{1-x}\text{Pt}_x$  alloy at  $x = 0.5$ , calculated by means of the single site KKR-CPA, becomes unstable at low temperatures, to a perturbation by a  $\langle 100 \rangle$  ordering wave and concluded that the corresponding long range ordered state (LRO) i.e. the  $L1_0$  structure should be the predicted ground state for which the large size mismatch between Ni and Pt plays the main role and the effect of relativity can be neglected. However, Lu *et al* [15] pointed out that a local ordering tendency determined by perturbation analysis, doesn't necessarily predict the correct LRO ground state if the size mismatch of the two elements is large, as is the case for Ni and Pt and concluded that relativity is the sole reason for long range order in NiPt. The work of Singh *et al* [16] demonstrated that the relativistic effects do stabilize the ordered structures over the disordered solid solution. Recently Ruban *et al* [17] have studied the problem of phase stability in NiPt alloy system based on ordered

calculations with the inclusion of Madelung energy with multipole corrections. In this paper, we examine the relativistic treatment of the Hamiltonian and charge transfer and lattice relaxation effects on the electronic structure and phase stability of face-centered cubic NiPt system at 25%, 50% and 75% of concentration of Pt. As mentioned already, the augmented space recursion (ASR) technique, which we use here, is capable of taking into account environmental effects, effects of short range order and local lattice relaxation effects due to size mismatches. To circumvent the problem of calculation of Madelung energy contribution for disordered system, we have used the appropriate effective atomic sphere radii for each of the constituents so that the spheres are neutral on the average and this has been done with precision at each concentration [18]. We have shown that without inclusion of relativistic effects the formation energy comes out to be positive which contradicts experimental results. With the scalar relativistic corrections, involving mass-velocity and Darwin terms, the formation energy comes out negative indicating that the relativistic effects play an important role in NiPt alloys in agreement with earlier studies. We find that the charge transfer effects have also an important role to play in deciding on the correct ground state structure, particularly when the concentration of Pt is high. Our study on transition temperatures based on a mean field theory could reproduce the qualitative experimental trends.

## 2. Formalism

### 2.1. The Effective Pair Interactions

We start from a completely disordered alloy. Each site  $R$  has an occupation variable  $n_R$  associated with it. For a homogeneous perfect disorder  $\langle n_R \rangle = x$ , where  $x$  is the concentration of one of the components of the alloy. In this homogeneously disordered system we now introduce fluctuations in the occupation variable at each site :  $\delta x_R = n_R - x$ . Expanding the total energy in this configuration about the energy of the perfectly disordered state we get :

$$E(x) = E^{(0)} + \sum_{R=1}^N E_R^{(1)} \delta x_R + \sum_{RR'=1}^N E_{RR'}^{(2)} \delta x_R \delta x_{R'} + \dots \quad (1)$$

The coefficients  $E^{(0)}$ ,  $E_R^{(1)}$  ... are the effective renormalized cluster interactions.  $E^{(0)}$  is the energy of the averaged disordered medium. The renormalized pair interactions  $E_{RR'}^{(2)}$  express the correlation between two sites and are the most dominant quantities for the analysis of phase stability. We will retain terms up to pair interactions in the configuration energy expansion. Higher order interactions may be included for a more accurate and complete description. For the phase stability study it is the pair interaction which plays the dominant role.

The total energy of a solid may be separated into two terms : a one-electron band contribution  $E_{BS}$  and the electrostatic contribution  $E_{ES}$ . The renormalized cluster interactions defined in (1) should, in principle, include both  $E_{BS}$  and  $E_{ES}$  contributions.

Since the renormalized cluster interactions involve the difference of cluster energies, it is usually assumed that the electrostatic terms cancel out and only the band structure contribution is important. Such an assumption which is not rigorously true, has been shown to be approximately valid in a number of alloy systems [19]. Considering only band structure contribution, the effective pair interactions may be written as :

$$E_{RR'}^{(2)} = - \int_{-\infty}^{E_F} dE \left\{ -\frac{1}{\pi} \Im m \log \sum_{IJ} \det \left( G^{IJ} \right) (E) \xi_{IJ} \right\} \quad (2)$$

where,  $G^{IJ}$  represents the configurationally averaged Green function corresponding to the disordered Hamiltonian whose R and R' sites are occupied by I-th and J-th type of atom, and

$$\xi_{IJ} = \begin{cases} +1 & \text{if } I=J \\ -1 & \text{if } I \neq J \end{cases}$$

The behavior of this function is quite complicated and hence the integration by standard routines (e.g. Simpson's rule or Chebyshev polynomials) is difficult, involving many iterations before convergence is achieved. Furthermore the integrand is multi-valued, being simply the phase of  $\sum_{IJ} \det \left( G^{IJ} \right) \xi_{IJ}$ . The way out for this was suggested by Burke [11] which relies on the repeated application of the partition theorem on the Hamiltonian  $H^{IJ}$ . The final result is given simply in terms of the zeroes and poles of the Green function in the region  $E < E_F$

$$E_{RR'}^{(2)} = 2 \sum_{IJ} \xi_{IJ} \sum_{k=0}^{\ell_{max}} \left[ \sum_{j=1}^{z_j^{k,IJ}} Z_j^{k,IJ} - \sum_{j=1}^{p_j^{k,IJ}} P_j^{k,IJ} + \left( p^{k,IJ} - z^{k,IJ} \right) E_F \right] \quad (3)$$

where  $Z_j^{k,IJ}$  and  $P_j^{k,IJ}$  are the zeros and poles of the peeled Green's function  $G_k^{IJ}$  of disordered Hamiltonian with occupancy at sites R and R' by I and J of which first (k-1) rows and columns has been deleted.  $p^{k,IJ}$  and  $z^{k,IJ}$  are the number of poles and zeroes in the energy region below  $E_F$ . The factor 2 accounts for the spin degeneracy.

## 2.2. The Augmented Space Recursion

As discussed in the previous section, the calculation of the effective pair interaction in our formalism reduces to the determination of the peeled configuration averaged green functions  $\langle G_k^{IJ} \rangle$ . We shall employ the augmented space recursion coupled with the linearized tight-binding muffin tin orbital method (TB-LMTO) introduced by Andersen and Jepsen [20] for a first principles determination of these configuration averaged quantities. We shall take the most localized, sparse tight binding first order Hamiltonian derived systematically from the LMTO theory within the atomic sphere approximation (ASA) and generalized to random alloys. The augmented space recursion method has been described at great length in earlier communications ([6]-[9], [12],[21],[22]). We refer the readers to these references for the details. We shall give here the final form of the effective Hamiltonian used for recursion in augmented space for the calculation of the peeled Green functions :

$$\begin{aligned}
H_k^{IJ} &= \sum_{\ell=k}^{\ell_{max}} C_{R,\ell}^I a_R^\dagger a_R + \sum_{\ell=1}^{\ell_{max}} C_{R',\ell}^J a_{R'}^\dagger a_{R'} + \sum_{R'' \neq R, R'} \sum_{\ell=1}^{\ell_{max}} \left( C_{R'',\ell}^B + \delta C_\ell \widetilde{\mathbf{M}}^{R''} \right) a_{R''}^\dagger a_{R''} + \dots \\
&+ \sum_{R'' \neq R} \sum_{\ell=k}^{\ell_{max}} \sum_{\ell'=1}^{\ell_{max}} \Delta_{R,\ell}^{1/2,I} S_{\ell,\ell'}^{R,R''} \left( \Delta_{R'',\ell'}^{1/2,B} + \delta \Delta_{\ell'}^{1/2} \widetilde{\mathbf{M}}^{R''} \right) a_R^\dagger a_{R''} + \dots \\
&+ \sum_{R'' \neq R'} \sum_{\ell=1}^{\ell_{max}} \sum_{\ell'=1}^{\ell_{max}} \Delta_{R',\ell}^{1/2,I} S_{\ell,\ell'}^{R',R''} \left( \Delta_{R'',\ell'}^{1/2,B} + \delta \Delta_{\ell'}^{1/2} \widetilde{\mathbf{M}}^{R''} \right) a_{R'}^\dagger a_{R''} + \dots \\
&+ \sum_{R'' \neq R} \sum_{\ell=1}^{\ell_{max}} \sum_{\ell'=k}^{\ell_{max}} \left( \Delta_{R'',\ell}^{1/2,B} + \delta \Delta_\ell^{1/2} \widetilde{\mathbf{M}}^{R''} \right) S_{\ell,\ell'}^{R'',R} \Delta_{R,\ell'}^{1/2,I} a_{R''}^\dagger a_R + \dots \\
&+ \sum_{R'' \neq R'} \sum_{\ell=1}^{\ell_{max}} \sum_{\ell'=1}^{\ell_{max}} \left( \Delta_{R'',\ell}^{1/2,B} + \delta \Delta_\ell^{1/2} \widetilde{\mathbf{M}}^{R''} \right) S_{\ell,\ell'}^{R'',R'} \Delta_{R',\ell'}^{1/2,I} a_{R''}^\dagger a_{R'} + \dots \\
&+ \sum_{R'' \neq R, R'} \sum_{R''' \neq R, R'} \sum_{\ell=1}^{\ell_{max}} \sum_{\ell'=1}^{\ell_{max}} \left( \Delta_{R'',\ell}^{1/2,B} + \delta \Delta_\ell^{1/2} \widetilde{\mathbf{M}}^{R''} \right) S_{\ell,\ell'}^{R'',R'''} \left( \Delta_{R''',\ell'}^{1/2,B} + \delta \Delta_{\ell'}^{1/2} \widetilde{\mathbf{M}}^{R'''} \right) \dots \\
&\dots \left( a_{R''}^\dagger a_{R'''} + a_{R'''}^\dagger a_{R''} \right) \tag{4}
\end{aligned}$$

For a binary distribution  $\widetilde{\mathbf{M}}^R$  is given by:

$$\widetilde{\mathbf{M}}^R = x b_{R\uparrow}^\dagger b_{R\uparrow} + (1-x) b_{R\downarrow}^\dagger b_{R\downarrow} + \sqrt{x(1-x)} \left( b_{R\uparrow}^\dagger b_{R\downarrow} + b_{R\downarrow}^\dagger b_{R\uparrow} \right) \tag{5}$$

For non-isochoric alloys, the difference in atomic radii of the constituents lead to change in the electronic density of states, as confirmed by experiment [23] and approximate theoretical techniques [24]. One thus expects that the mismatch of size produces, in addition to a relaxation energy  $E_R$  contribution, a change in the band structure. Within our Augmented Space Recursion (ASR), off-diagonal disorder in the structure matrix  $S^\beta$  because of local lattice distortions due to size mismatch of the constituents, can be handled on the same footing as diagonal disorder in the potential parameters [22].

The augmented space recursion with the TB-LMTO Hamiltonian coupled with orbital peeling allows us to compute configuration averaged pair-potentials directly, without resorting to any direct averaging over a finite number of configurations. In an earlier communication [7] we have discussed how one uses the local symmetries of the augmented space to reduce the Hamiltonian and carry out the recursion on a reducible subspace of much lower rank. If we fix the occupation of two sites, the local symmetry of the augmented space is lowered (this is very similar to the lowering of spherical symmetry to cylindrical symmetry when a preferred direction is introduced in an isotropic system). We may then carry out the recursion in a suitably reduced subspace.

### 2.3. Static concentration wave method

The static concentration wave (SCW) was proposed as a theory for ordering by Khachatryan ([25],[26]). The occupation probability  $n(\vec{r})$  plays the key role in this

theory. This function  $n(\vec{r})$  that determines the distribution of solute atoms in an ordered phase can be represented as a superposition of concentration waves:

$$n(\vec{r}) = c + \frac{1}{2} \sum_j [Q(\vec{k}_j) \exp(i\vec{k}_j \cdot \vec{r}) + Q^*(\vec{k}_j) \exp(-i\vec{k}_j \cdot \vec{r})] \quad (6)$$

where  $\exp(i\vec{k}_j \cdot \vec{r})$  is a static concentration wave,  $\vec{k}_j$  is a non zero wave vector defined in the first Brillouin zone of the disordered alloy,  $\vec{r}$  is a site vector of the lattice  $\{\vec{r}\}$ , index  $j$  denotes the wave vectors in the Brillouin zone,  $Q(\vec{k}_j)$  is static concentration wave amplitude and  $c$  is the atomic fraction of the alloying element.

The study of phase stability requires accurate approximations to the configurational energy as well as the use of statistical models to obtain the configurational entropy. The configurational energy within the pair interaction can be represented in Fourier space as the product of the Fourier transform of the effective pair interaction  $V(\vec{k})$  and that of the pair correlation function  $Q(\vec{k})$ :

$$E \simeq \left(\frac{N}{2}\right) \sum_{\vec{k}} V(\vec{k})Q(\vec{k})$$

where  $N$  is the number of atoms. Minimization of  $E$  will naturally occur for states of order characterized by maxima in the  $Q(\vec{k})$  pair correlation spectrum located in the regions of the absolute minima of  $V(\vec{k})$ . Consequently, much can be predicted about the types of ordering to be expected from a study of the shape of  $V(\vec{k})$ , particularly from a search of its absolute minima (special points). At these points,

$$|\nabla_h V(h)| = 0$$

This was pointed out by Lifshitz [27, 28] and Khachaturyan [25, 26]. Different types of ordered structures can be related directly to the minima of  $V(\vec{k})$ . In other words, given the knowledge of concentration wave vectors, one can readily predict the most stable ordered structure of the system at low temperatures. This is comparable to the knowledge derived from the studies like those based on X-ray, electron and neutron diffraction. A peak at the  $\Gamma$  point,  $\vec{k} = (000)$ , indicates the phase separation, while a peak at the  $\Gamma$  point,  $\vec{k} = (100)$ , in a fcc lattice suggests ordering. Peaks away from special points may correspond to the formation of long period superstructures. With in a simple mean field approximation, the instability can be obtained in the following way: If we add the expression for dominant quadratic term in the average energy to that of the configurational entropy under the simple mean field approximation we obtain an expression for the free energy:

$$F = \sum_{i,j} V_{ij}^2 (n_i - c)(n_j - c) + k_B T \sum_i [n_i \ln n_i + (1 - n_i) \ln(1 - n_i)]$$

where  $n_i$  is the concentration of the species A at the  $i$ -th site and  $c$  is the average concentration of that species. If we define a configuration variable  $\gamma_i^0$  as  $\langle \delta n_i \rangle_0$  (the symbol  $\langle \dots \rangle_0$  denotes micro-canonical averaging), which is the variable relevant to the

stability analysis, then the harmonic term in the Taylor expansion of the above free energy is

$$F^2 = \frac{N}{2} \sum_h \Gamma^*(\vec{k}(h)) F(\vec{k}(h)) \Gamma(\vec{k}(h)) \quad (7)$$

where,  $\vec{k}(h) = 2\pi h_\alpha \vec{b}_\alpha$  and  $\Gamma(\vec{k}(h)) = \mathcal{F}(n(\vec{r}) - c)$ . The stability of a solid solution with respect to a small concentration wave of given wave vector  $\vec{k}(h)$  is guaranteed as long as  $F(\vec{k}(h))$  is positive definite. Instability sets in when  $F(\vec{k}(h))$  vanishes i.e.

$$F(\vec{k}(h)) = k_B T^i + V(\vec{k}(h)) c (1 - c) = 0 \quad (8)$$

$T^i$  being the temperature at which the instability sets in for the considered concentration wave. It appears from the above expression that under a simple mean field approximation the spinodal is always a parabola in the  $(t, c)$  phase diagram, symmetric about  $x = 0.5$ . It is the concentration dependence of the effective pair interactions which brings about the asymmetry.

### 3. Computational details

#### 3.1. Convergence of augmented space recursion

The effective pair potentials are calculated at the Fermi level so one needs to be very careful about the convergence of the Fermi energy as well as that of the effective pair potentials. In fact, errors can arise in the augmented space recursion because one can carry out only finite number of recursion steps and then terminate the continued fraction using available terminators. Also one chooses a large but finite part of the augmented space nearest neighbour map and ignores the part of the augmented space very far from the starting state. This is also a source of error.

For finding out the Fermi energy accurately, we have used the energy dependent version of augmented space recursion. In this version of ASR the defining Hamiltonian is recast into an energy dependent Hamiltonian having only diagonal disorder. We then choose a few seed points across the energy spectrum uniformly, carry out recursion on those points and spline fit the coefficients of recursion through out the whole spectrum. This enables us to carry out large number of recursion steps since the configuration space grows significantly less faster for diagonal as compared with off diagonal disorder. For details see ref [29]

We have checked the convergence of Fermi energy and effective pair potentials with respect to recursion steps and the number of seed energy points taking the case of NiPt<sub>3</sub> system. We have found that the Fermi energy and effective pair potentials converge beyond seven recursion steps and thirty five seed energy points. In our all calculations reported in the following have been carried out with eight recursion steps and thirty five seed energy points.

### 3.2. Antiphase boundary energy

Kanamori and Kakehasi [30] used the method of geometrical inequalities which is capable of searching for ground structure. They considered the energy of the three dimensional Ising like model:

$$E_c = \sum_k V_k P_k \quad (9)$$

where,  $V_k$  is the interaction constant of the K-th nearest neighbour interaction and  $P_k$  is the total number of  $k^{th}$  neighboring pairs in the given configuration. Defining the anti-phase boundary energy  $\xi$  by

$$\xi = -V_2 + 4 V_3 - 4 V_4 , \quad (10)$$

the authors proved rigorously that for  $\xi > 0$   $L1_2$  and  $L1_0$  are the corresponding superstructures possible at concentration 25 % and 50 % while for  $\xi < 0$ , one has the  $DO_{22}$  and  $A_2B_2$  superstructures. We have applied these conditions in our calculations to find out the relative stability between  $DO_{22}$  and  $L1_2$  structures in  $Ni_3Pt$  and  $NiPt_3$  that between  $A_2B_2$  and  $L1_0$  in  $NiPt$ .

### 3.3. Special-point ordering

A wide range of phenomena related to order-disorder and magnetic transitions can be explained using the symmetry properties of the pair potentials ( $V_{ij}$ ). If a symmetry element (rotation, rotation-inversion or mirror plane) of the space group in  $\mathbf{k}$ -space is located at point  $h$ , the vector representing the gradient  $\nabla_h V(h)$  of an arbitrary potential energy function  $V(h)$  at that point must lie along or within the symmetry element. If two or more symmetry elements intersect at point  $h$ , one must necessarily have

$$|\nabla_h V(h)| = 0 \quad (11)$$

since a finite magnitude vector can not lie simultaneously in intersecting straight lines having only a point in common. At these so-called special points, the potential energy function  $V(h)$  represent an extremum regardless of the choice of the pair interaction energies. Thus special points play an important role in the search for lowest energy ordered structures. The points which differ by a vector of a reciprocal lattice are considered equivalent. In the case of simple structures with a single atom per unit cell, it is sufficient that two symmetry elements intersect at special points. These special points are listed in Crystallographic tables. They are always located at the surface of the Brillouin zone. The ‘star’ of a special point vector  $\mathbf{k}$  is obtained by applying all the rotations and rotation-inversion of the space group on the vector  $\mathbf{k}$ . All these vectors of a star are also considered equivalent. The special points of the  $fcc$  structure are located at the points  $\Gamma$ , X, W and L of the Brillouin zone as shown in table 1.

### 3.4. Ordering energy

The ordering energy is defined as the difference between the formation energy of ordered alloy and the corresponding formation energy of disordered alloy. Since we are dealing

**Table 1.** The special points and stars of the *fcc* structure

<b>k</b> -vector Star	Members	Brillouin zone points	Ordering structure
$\langle 000 \rangle$	[000]	$\Gamma$	
$\langle 100 \rangle$	[100] [010] [001]	X	$L1_2, L1_0$
$\langle 1\frac{1}{2}0 \rangle$	$[1\frac{1}{2}0]$ $[\frac{1}{2}01]$ $[01\frac{1}{2}]$ $[\bar{1}\frac{1}{2}0]$ $[\frac{1}{2}0\bar{1}]$ $[0\bar{1}\frac{1}{2}0]$	W	$A_2B_2, DO_{22}$
$\langle \frac{1}{2}\frac{1}{2}\frac{1}{2} \rangle$	$[\frac{1}{2}\frac{1}{2}\frac{1}{2}]$ $[\frac{1}{2}\frac{1}{2}\bar{\frac{1}{2}}]$ $[\frac{1}{2}\frac{1}{2}\frac{1}{2}]$ $[\frac{1}{2}\frac{1}{2}\frac{1}{2}]$	L	$L1_1$

with the effective pair potentials, the ordering energy can be calculated using these pair potentials. The relation for ordering energy using pair potentials is given as :

$$E^{ord} = \frac{1}{2} \sum_k V_k \delta x_o \delta x_k \quad (12)$$

where,  $\delta x_o$  ( $\delta x_k$ ) =  $x_o$  ( $x_k$ ) -  $x$ ,  $x_o$  ( $x_k$ ) = 1 if the site  $o/k$  is occupied by A atom and  $x_o$  = 0 if the site  $o/k$  is occupied by B atom. For  $L1_2$  structure (for  $Ni_3Pt$  and  $NiPt_3$  in our case) the expression for ordering energy per atom in terms of pair potentials considering only up to fourth nearest neighbours is given as:

$$E_{Ni_3Pt}^{ord} = -\frac{3}{32}[V_1 - \frac{1}{3} V_2 + V_3 - \frac{1}{3} V_4] \quad (13)$$

For  $L1_0$  structure for NiPt the expression for ordering energy per atom considering up to fourth nearest neighbour pair potentials is given as:

$$E_{NiPt}^{ord} = -\frac{1}{8}[V_1 - V_2 + V_3 - V_4] \quad (14)$$

Using these two relations we have found the ordering energy for  $Ni_3Pt$ , NiPt and  $NiPt_3$ .

#### 4. Results and discussions

We have applied our formalism discussed in the previous section in calculating the effective pair potentials for the fcc based NiPt alloys for concentrations  $x = 0.25, 0.5$  and  $0.75$  of Pt. The calculation of the effective pair potentials has been restricted up to fourth nearest neighbour interactions. Total energy density functional calculations were performed at the concentration  $x = 0.25, 0.5$  and  $0.75$  of Pt. The Kohn-Sham

**Table 2.** The calculated equilibrium lattice parameters with the choice of neutral charge spheres including scalar relativistic corrections. The corresponding lattice parameters with out relativistic corrections are given in brackets.

concentration of Pt	eq. lattice parameter in au. SR(NR)
0.00(Ni)	6.528(6.568) (expt. 6.66)
0.25(Ni <sub>3</sub> Pt)	6.758(6.890)
0.50(NiPt)	7.127(7.335)
0.75(NiPt <sub>3</sub> )	7.196(7.467)
1.00(Pt)	7.3685(7.683) (expt. 7.41)

equations were solved in the local density approximation (LDA). The LDA was treated with in the context of linear muffin tin orbitals in the atomic sphere approximation. The calculations were performed non relativistically as well as scalar relativistically and the exchange correlation potential of Von Barth and Hedin was used. Two sets of calculations were performed one with the same Wigner-Seitz radius (charged spheres) for Ni and Pt. In other set we followed the procedure described by Kudrnovský *et al* [18] and used an extension of the procedure proposed by Andersen *et al* [20], which allows us flexibility in the choice of ASA radii for the constituents. The idea is to choose ASA radii of atomic species in such a way that the spheres are charge neutral on the average. The potential parameters  $\Delta_I^I$  and  $\gamma_I^I$  of the constituent I were then scaled by the factors  $(s^I/s^{alloy})^{2l+1}$  to account for the fact that the Wigner-Seitz radius of constituent I,  $s^I$ , is different from that of the alloy,  $s^{alloy}$ . These potential parameters were used to parameterize the alloy Hamiltonian. For the purpose of augmented space recursion, seven shell map was generated and thirty five seed energy point recursion was performed, as explained in previous section, to calculate the Fermi energy with the second order LMTO-ASA Hamiltonian through the recursion method using eight level of recursion and analytical terminator of Luchini and Nex. For the effective pair potentials, we used the orbital peeling method within the frame work of ASR for the calculation of peeled averaged Green function described in detail in the earlier section.

In table 2, we have quoted the equilibrium lattice parameters that were used in our calculations. We obtained these by minimizing the total energies with respect to the lattice parameters. We have got slightly lower equilibrium lattice parameters as compared to experimental ones. This is characteristic of the local density approximation which overestimates bonding.

In figure 1 we have shown the formation energy of NiPt alloy system with various Pt concentrations based on ordered calculations. It shows that without inclusion of relativistic effects the formation energy comes out to be positive which contradicts experimental results. With the inclusion of scalar relativistic corrections the formation energy comes out to be negative. This indicates that relativistic effects play an important

**Table 3.** Formation energies for  $\text{Ni}_x\text{Pt}_y$  with the choice of neutral charge spheres including scalar relativistic correction. The values in brackets are without relativistic correction. The corresponding estimate for charged sphere calculations are shown with \*'s. \*\* refers to calculations with out combined correction. \*\*\* refers to disordered formation energy

$y$	This work SR(NR)	Expt.[31]	FPLMTO+ CWM[31]	LMTO [31]	LMTO+ CWM[32]	KKR-ASA (KKR-CPA)
0.25	-7.50(4.25) -7.59*(4.17)*	-5.16	-6.30	-7.17	-6.66	
0.50	-9.44(4.74) -9.02*(4.85)*	-7.06	-8.69	-8.5	-8.95	-12.00** [16] -8.10 [34] (-7.7***)[16]
0.75	-8.15(4.22) -3.97*(6.65)*	-4.78	-6.40	-6.70	-9.12	

role in the stability of NiPt alloys, in agreement with earlier studies. Our results are in closer agreement with previous works based on the Full-Potential LMTO and the Connolly-Williams technique ([31],[32],[33]) and with experimental estimate. Singh *et al* [16] have also calculated the formation energy for 50% of Pt. Their results for the formation energy obtained from ordered calculations without combined correction deviates quite a bit from ours as well as other results based on the Full-Potential LMTO and the Connolly-Williams technique ([31],[32],[33]), which is presumably due to the neglect of the combined correction in reference [16]. Singh *et al* [34] have also done the calculation with combined correction which shows better agreement. The full-potential methods are expected to provide better estimates than other methods.

We next approached the problem from the disordered end. We start from a completely disordered alloy and set up concentration wave fluctuations in it to see when this destabilizes the disordered phase as suggested by Khachatryan [25]. We have computed the effective pair potentials for two sets of potential parameters with charged and charge neutral spheres. Figure 2 shows that the effective pair potentials for NiPt<sub>3</sub> is very small in magnitude using potential parameters with charged spheres. We even used these pair potentials and calculated the anti-phase boundary energy according to the prescription described in the previous section. The anti-phase boundary energy comes out to be negative for NiPt<sub>3</sub> and NiPt indicating stability of DO<sub>22</sub> over L1<sub>2</sub> for NiPt<sub>3</sub> and A<sub>2</sub>B<sub>2</sub> over L1<sub>0</sub> for NiPt. Further we calculated the minima of the special points according to the prescription described in the previous section. In the case of NiPt<sub>3</sub> and NiPt shown in figure 4, we could not get the minima at  $\langle 100 \rangle$  which is not quite correct because

**Table 4.** The effective pair potentials for NiPt alloy system calculated with potential parameters taken from calculations with the choice of charged spheres and including scalar relativistic correction. (O-L) refers to calculations without multipole corrections, M refers to calculations with multipole corrections and SCI to calculations with screened Coulomb interactions. US-PP refers to ultrasoft pseudo-potentials. \* refers to non-relativistic calculations.

Reference	$v_1$ (mRy/atom)	$v_2$ (mRy/atom)	$v_3$ (mRy/atom)	$v_4$ (mRy/atom)
<b>Concentration of Pt = 25%</b>				
Present work	11.36	-0.05	-0.07	-0.41
	11.972*	0.015*	0.054*	0.046*
<b>Concentration of Pt = 50%</b>				
Present work	7.832	0.114	-0.129	-0.057
	8.597*	0.10*	0.053*	0.263*
Singh <i>et al</i> [16]	4.22	1.14	0.22	-1.04
	4.94*	0.52*	0.32*	-0.18*
Pinski <i>et al</i> [14]	9.4*	0.8*	0.4*	-0.2*
Pourovskii <i>et al</i> [37] CWM-ASA+M SGPM	5.00	0.25	0.19	-0.28
	5.28	0.06	-0.82	-0.66
Ruban <i>et al</i> [17] with SGPM ASA+M (O-L)(SCI) ASA (SCI)	14.05(15.44)	0.32(-0.10)	-1.09(-1.22)	-1.76(-0.84)
	12.26(14.35)	0.53(-0.15)	-1.31(-1.48)	-2.14(-0.98)
With Connolly Williams ASA+M ASA+M (O-L) ASA	12.68	1.31	-0.02	-0.73
	13.70	0.49	-0.86	-1.39
US(PP) Direct calculation(SCI) ASA+M	14.33	0.28	-1.72	-1.92
	12.81	1.30	0.69	-0.40
	12.45	0.47	-0.49	-0.65
<b>Concentration of Pt = 75%</b>				
Present work	2.785	0.236	-0.116	0.276
	3.813*	0.361*	-0.175*	0.366*

**Table 5.** The effective pair potentials for NiPt alloys with potential parameters taken from calculations with the choice of charge neutral spheres including scalar relativistic corrections. The corresponding estimate for non relativistic calculations are shown with \*'s.

Reference	$v_1$ (mRy/atom)	$v_2$ (mRy/atom)	$v_3$ (mRy/atom)	$v_4$ (mRy/atom)
<b>Concentration of Pt = 25%</b>				
Present work	12.34	-0.092	-0.046	-0.54
	13.08*	-0.021*	0.152*	-0.041*
<b>Concentration of Pt = 50%</b>				
Present work	10.08	0.1	0.004	-0.24
	10.111*	0.126*	0.246*	0.175*
Singh <i>et al</i> [16]	16.02	1.34	0.06	-1.58
	11.96*	0.66*	0.28*	-0.46*
Ruban <i>et al</i> [17] Neutral(GPM)	5.49	1.22	0.01	-0.73
<b>Concentration of Pt = 75%</b>				
Present work	8.9	0.26	0.1	0.02
	7.874*	0.297*	0.276*	0.34*

experiments show NiPt<sub>3</sub> has  $L_{12}$  and NiPt has  $L_{10}$  ordering. But in the case of Ni<sub>3</sub>Pt we could get the positive anti-phase boundary energy as well as minima at  $\langle 100 \rangle$  correctly showing the ordering  $L_{12}$ . In figure 3 we have plotted the effective pair potentials as a function of energy relative to Fermi energy and number of neighboring shells with charge neutral potential parameters including scalar relativistic correction which shows that the first nearest neighbor pair potentials are larger in magnitude than the second, third and fourth nearest neighbour pair potentials. With potential parameters from neutral sphere calculations including scalar relativistic correction for NiPt<sub>3</sub> and NiPt the anti-phase boundary energies come out to be positive and the minima of special points are at  $\langle 100 \rangle$  correctly showing  $L_{12}$  and  $L_{10}$  orderings. If we use charge neutral potential parameters without including scalar relativistic effect the anti-phase boundary energies come out to be positive for Ni<sub>3</sub>Pt and NiPt but negative for NiPt<sub>3</sub>. This shows for NiPt<sub>3</sub> both scalar relativistic as well as charge transfer effects play important role to predict correct ground state.

So, we argue that on increasing the concentration of Pt atom the careful treatment to take into account of charge transfer effect becomes increasingly important. In figure 3, we have also shown the effective pair potentials without scalar relativistic corrections. For NiPt<sub>3</sub> it is clearly seen that the effective pair potentials with scalar relativistic

**Table 6.** The anti-phase boundary energies for  $\text{Ni}_x\text{Pt}_y$  alloys from charged and neutral sphere calculations

concentration of Pt	APB energy (mRy/atom)	
	Charged spheres	Neutral spheres
	Relativistic(Non-Relativistic)	
0.25	1.41(0.017)	2.07(0.793)
0.50	-0.402(-0.94)	0.876(0.158)
0.75	-1.804(-2.525)	0.06(-0.553)

correction are larger in magnitude than the non relativistic ones which is expected because of higher concentration of Pt.

In figure 5 we have plotted that the effective pair potentials vs concentration of Pt with charge neutral potential parameters including scalar relativistic correction which shows that the first nearest neighbour effective pair potentials decrease with the increase of the Pt concentration. Singh *et al* [16, 35] have also calculated the effective pair potentials using KKR-CPA-GPM method. Their values of effective pair potentials are much larger than ours. They pointed out that due to the large values of effective pair potentials the ordering energy and ordering temperatures (transition temperatures) are much higher than that observed experimentally. Our estimates give rise to instability temperatures which are closer to the experimental results (shown in figure 6). For example, our estimate for the instability temperature for the 50% alloy is 1683°K, whereas the estimate from the KKR-CPA is around 2979°K. The experimental estimates of the transition temperature is 950°K [36]. In KKR-CPA-GPM method one considers only the single site approximation and one does not take into account any off diagonal disorder which may arise because of size mismatch of the constituent atoms. The ASR, on the other hand, as discussed earlier can do this with facility. Furthermore, Singh *et al* [16, 35] in their calculation for charge neutrality have taken the ratio of Wigner Seitz radii of Ni and Pt as 0.95. We, on the other hand, have varied the ratio, with the provision that the total volume is conserved, till, on the average, the spheres become charge neutral. We have observed the ratio to be 0.909, 0.913 and 0.919 for the  $\text{Ni}_3\text{Pt}$ ,  $\text{NiPt}$  and  $\text{NiPt}_3$ . Given these differences, it is not surprising that our calculations result in smaller values of the pair-potentials leading to better estimates of the instability temperatures. The calculations of Pinski *et al* [14] were carried out without scalar relativistic effects. Their values are consequently rather large as compared to ours. Ruban *et al* [17] have calculated pair potentials for 50% concentration of Pt using different methods and showed that different methods give different values of pair potentials. Their nearest neighbor pair-potential is slightly higher than ours which could be due to the effect of lattice distortion which is taken care of in our methodology. The

effective pair potentials obtained by Pourovskii *et al* [37] from the neutral charge spheres GPM method are similar to the estimates of Ruban *et al* [17].

In figure 6 we have shown the ordering energy, anti-phase boundary energy and instability temperatures vs concentration of Pt with charge neutral potential parameters including scalar relativistic correction. The ordering energy in all three cases Ni<sub>3</sub>Pt, NiPt and NiPt<sub>3</sub> is negative showing the stability of ordered structures compared to disordered solution. Among all three concentrations, NiPt attains maximum value of ordering energy which confirms that  $L1_0$  in NiPt system is the most stable structure. The anti-phase boundary energy in all these cases Ni<sub>3</sub>Pt, NiPt and NiPt<sub>3</sub> comes out to be positive showing the ordering structures  $L1_2$  for Ni<sub>3</sub>Pt,  $L1_0$  for NiPt and  $L1_2$  for NiPt<sub>3</sub> as described above. The magnitude of instability temperatures using the charge neutral potential parameters comes out to be larger than the experimental transition temperatures. However, the qualitative trend of the change of the instability temperatures with changing concentration of Pt is right. The calculated qualitative phase diagram (instability temperature vs concentration of Pt) shows asymmetric feature which is not observed experimentally. This could be due to the neglect of magnetism in the calculations of effective pair interactions which can have significant effect particularly in the high concentrations of Ni. Amador *et al* [31] also reported the phase diagram (instability temperature vs concentration of Pt) of this system described by the nearest neighbour tetrahedron effective interactions from clusters with appropriate effective volume. Their values for transition temperatures are smaller than ours but there is high asymmetry in their phase diagram and even the trend is not same as experimental findings.

## 5. Conclusion

Our total energy calculations for the ordered alloys indicate that in order to have the correct sign for the formation energy, it is essential to include relativistic corrections. Our analysis of the concentration wave approach indicates that for Ni<sub>3</sub>Pt neither relativistic correction nor the charge transfer effect is essential for the correct prediction of the  $L1_2$  ground state. For NiPt although scalar relativistic correction is not essential, careful treatment of charge transfer effect is a must to predict the correct ground state ( $L1_0$ ). For NiPt<sub>3</sub> both these corrections are essential to predict the correct ground state  $L1_2$ .

Although it seems that qualitatively the relativistic corrections and charge transfer effect plays the essential role only for the high Pt content alloys, for quantitative prediction of the instability temperature both these corrections are required across the concentration range.

The main conclusions of this paper are :

- We have demonstrated that for accurate prediction of the ground state structures and instability temperatures for alloys with components with large atomic size

differences like NiPt, it is essential to take into account both relativistic corrections and averaged charge neutrality of the atomic spheres.

- We have also demonstrated the augmented space recursion combined with the first-principles tight-binding linearized muffin-tin orbitals and the orbital peeling are both computationally feasible and suitable techniques for such studies as described above.

These techniques will form the basis of our further study into similar alloy systems, but with magnetic effects included.

## References

- [1] Gonis A., Zhang X. G., Freeman A. J., Turchi P., Stocks G. M. and Nicholson D. M., *Phys. Rev.* **B36** 4630 (1987)
- [2] Connolly J. W. D. and Williams A. R., *Phys. Rev.* **B27** 5169 (1983)
- [3] Ducastelle F. and Gautier F., *J. Phys. F: Met. Phys.* **F6** 2039 (1976)
- [4] Gonis A. and Garland J. W., *Phys. Rev.* **B16** 2424 (1977)
- [5] Dreyssé H., Berera A., Wills L. T. and de Fontaine D., *Phys. Rev.* **B39** 2442 (1989) ; Wolverton C., Ceder G., de Fontaine D. and Dreyssé H., *Phys. Rev.* **B48** 726 (1993)
- [6] Saha T., Dasgupta I. and Mookerjee A., *J. Phys.: Condens. Matter* **6** L245 (1995) ; Saha T. and Mookerjee A., *J. Phys.: Condens. Matter* **8** 2915 (1996) ; Dasgupta I., Saha T. and Mookerjee A., *Phys. Rev.* **B51** 17724 (1993)
- [7] Saha T., Dasgupta I. and Mookerjee A., *J. Phys. Condens. Matter.* **6** L245 (1994)
- [8] Haydock R., Heine V. and Kelly M. J., *J. Phys. C: Solid State Phys.* **C5** 2845 (1972) ; Haydock R. , *Solid State Physics* **35** (Academic Press, N. Y. ) (1988)
- [9] Ghosh S., Das N. and Mookerjee A., *J. Phys.: Condens. Matter* **9** 10701(1999) ; Chakrabarti A and Mookerjee A., *J. Phys.: Condens. Matter* **13** 10149(2001)
- [10] Saha T. and Mookerjee A., *J. Phys.: Condens. Matter* **8** 2915 (1996)
- [11] Burke N. R. , *Surf. Sci.* **58** 349 (1976)
- [12] Saha T., Ph.D. Thesis, Jadavpur University, (1995)
- [13] Treglia G. and Ducastelle F. *J. Phys.* **F17** 1935 (1987)
- [14] Pinski F.J., Ginatempo B., Johnson D.D., Staunton J.B., Stocks J.M. and Györffy B. L., *Phys. Rev. Lett.* **66** 776 (1991); **68** 1962 (1992)
- [15] Lu Z.W., Wei S.H. Wei, and Zunger A. *Phys. Rev. Lett.* **66** 1753 (1991), **68** 1961 (1992)
- [16] Singh P. P., Gonis A. and Turchi P.A.E *Phys. Rev. Lett.* **71** 1605 (1993)
- [17] Ruban A.V., Simak S. I., Korzhavyi P.A and Skriver H.L *Phys. Rev.* **B66** 024202 (2002)
- [18] Kudrnovský J. and Drchal V. , *Phys. Rev.* **B41** 7515 (1990)
- [19] Heine V., *Solid State Physics* **35** (Academic Press, N. Y. ) (1988)
- [20] Andersen O. K. and Jepsen O., *Phys. Rev. Lett.* **53** 2571 (1984)
- [21] Mookerjee A. , *J. Phys. C: Solid State Phys.* **C6** 1340 (1973)
- [22] Saha T. , Dasgupta I. and Mookerjee A. , *Phys. Rev.* **B51** 3413 (1995)
- [23] Wright H., Weightman P., Andrews P.T., Folkerts W., Flipse C.F.J., Sawatsky G.A., Norman D. and Padmore H., *Phys. Rev.* **B35** 519 (1987)
- [24] Bose S.K., Kudrnovský J., Jepsen O. and Andersen O.K., *Phys. Rev.* **B45** 8272 (1992)
- [25] Khachatryan A.G., *Prog. Mater. Sci.*, **22**, 1 (1978).
- [26] Khachatryan A.G. *Theory Of Structural Transformations In Solids* , Willey, New York (1983).
- [27] Landau L.D. and Lifshitz E.M. in *Statistical Physics*, Second and Third Editions, Part 1, (Pergamon Press, Oxford, 1969 and 1980).
- [28] Krivoglaz M.A. and Smirnov A.A in *The theory of Order-Disorder in Alloys*, (McDonald, London, 1964).

- [29] Ghosh S.D., Ph.D. Thesis, Jadavpur University, (2000)
- [30] Kanamori J., Kakehasi Y., *J Physique Colloq.* **38** C7-274 (1977)
- [31] Amador C., Lambrecht W.R.L., van Schilfgaarde M. and Segall B. *Phys. Rev.* **B47** 15276 (1993)
- [32] Ruban A.V., Abrikosov I.A, and Skriver H.L. *Phys. Rev.* **B51** 12958 (1995)
- [33] de Fontaine D., in *Solid State Physics*, (eds.) H. Ehrenreich, F. Seitz and D. Turnbull (Academic Press, New York, 1994), **Vol. 47** p.33.
- [34] Singh P. P., and Gonis A. *Phys. Rev.* **B49** 1642 (1994)
- [35] Singh P. P. , *Pramana* **47** 99 (1996)
- [36] Dahmani C.E., Cadeville, M.C., Sanchez J.M. and Moran-Lopez J. L. *Phys. Rev. Lett.* **55** 1208 (1985)
- [37] Pourovskii L.V., Ruban A.V., Abrikosov I. A., Vekilov Y. Kh. and Johansson *Phys. Rev.* **B64** 035421 (2001)

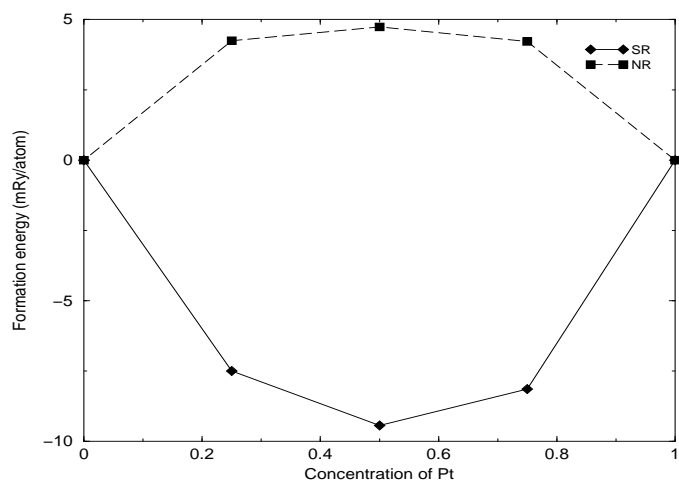


**Figure 1.** Formation energy vs concentration of Pt with the choice of neutral charge spheres

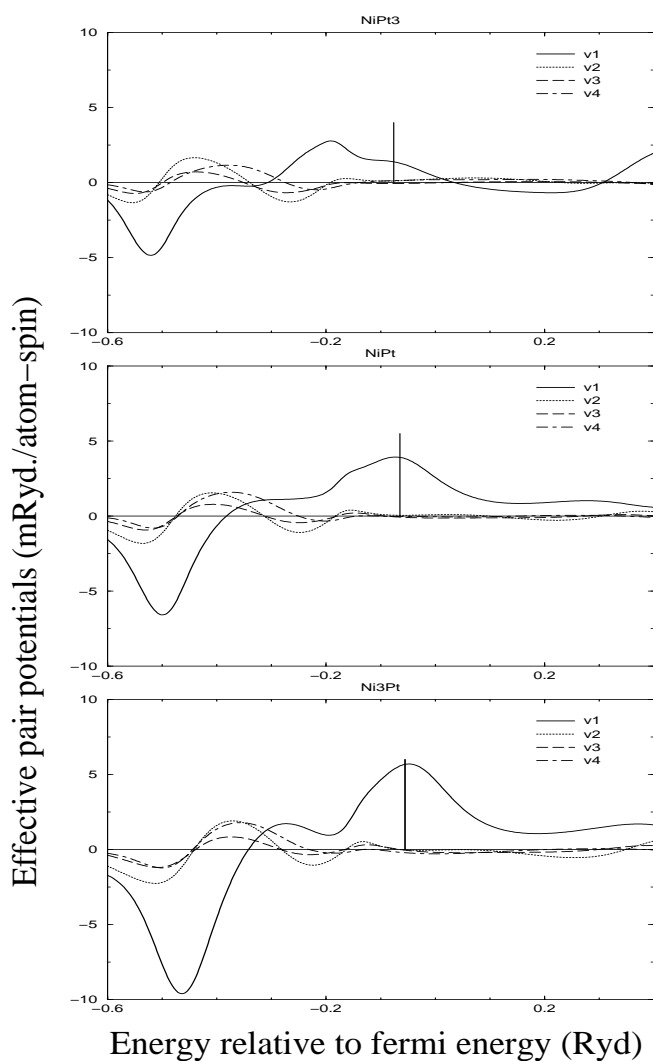


**Figure 2.** (i) The effective pair potentials with potential parameters taken from calculations with the choice of charged spheres including scalar relativistic corrections.

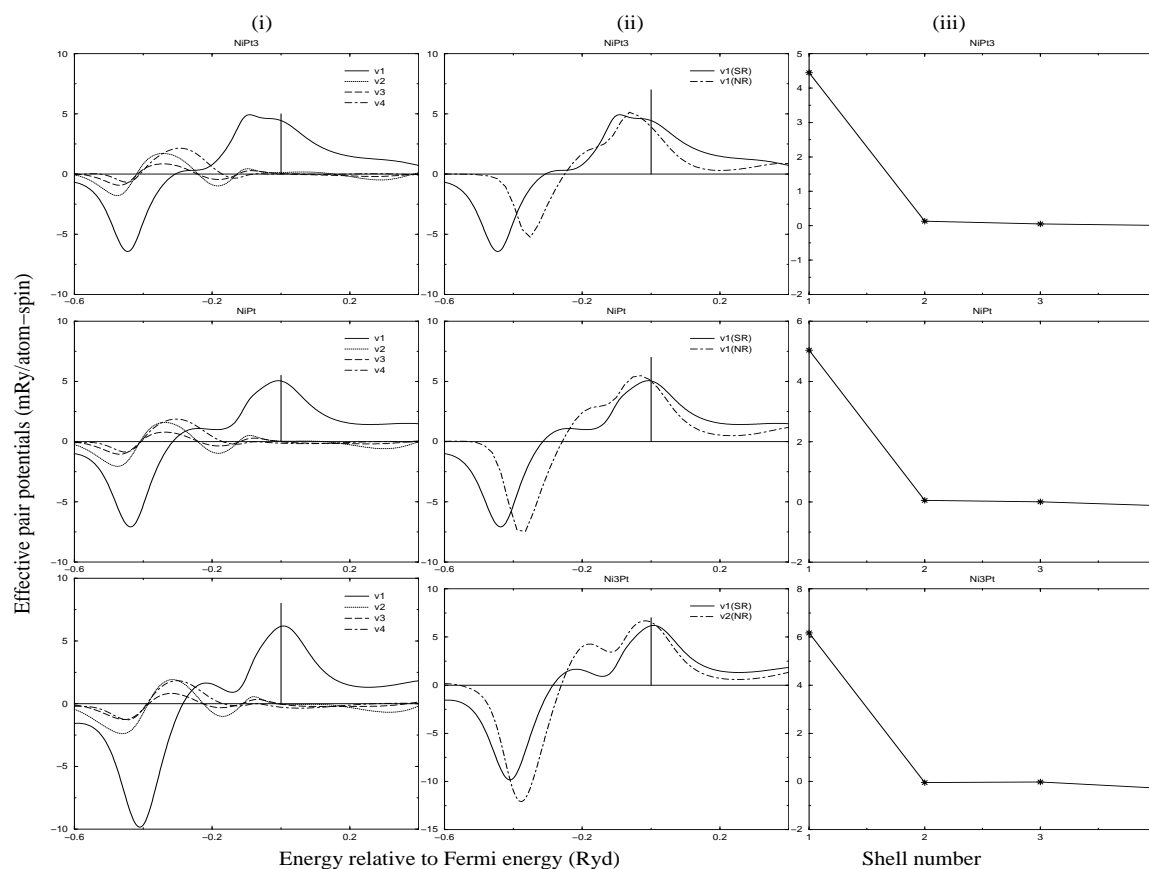


**Figure 3.** (i) The effective pair potentials as a function of energy relative to Fermi energy with charge neutral potential parameters including scalar relativistic corrections. (ii) Comparison between the first nearest neighbour effective pair potentials with scalar relativistic corrections and without scalar relativistic corrections by taking charge neutral potential parameters. (iii) The effective pair potentials as a function of shell numbers with charge neutral potential parameters including scalar relativistic correction.

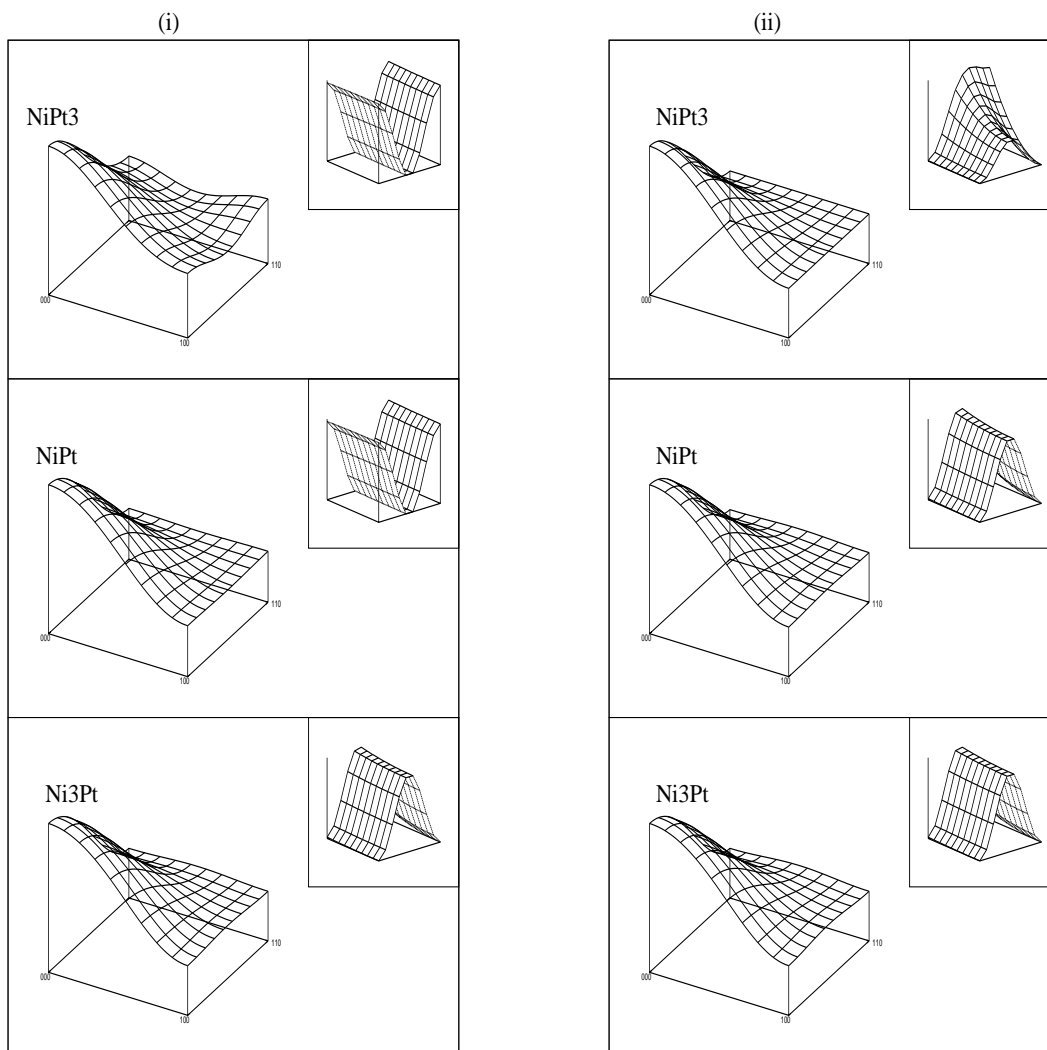


**Figure 4.** The  $V(\vec{k})$  surface for NiPt alloy system with potential parameters calculated with the choice of (i) charged spheres (ii) charge neutral spheres, on  $k_z = 0$  plane. The figures in inset are corresponding rescaled  $V(\vec{k})$  surfaces on  $k_z = 0$  plane along the (100) to (110) direction to view the minima.

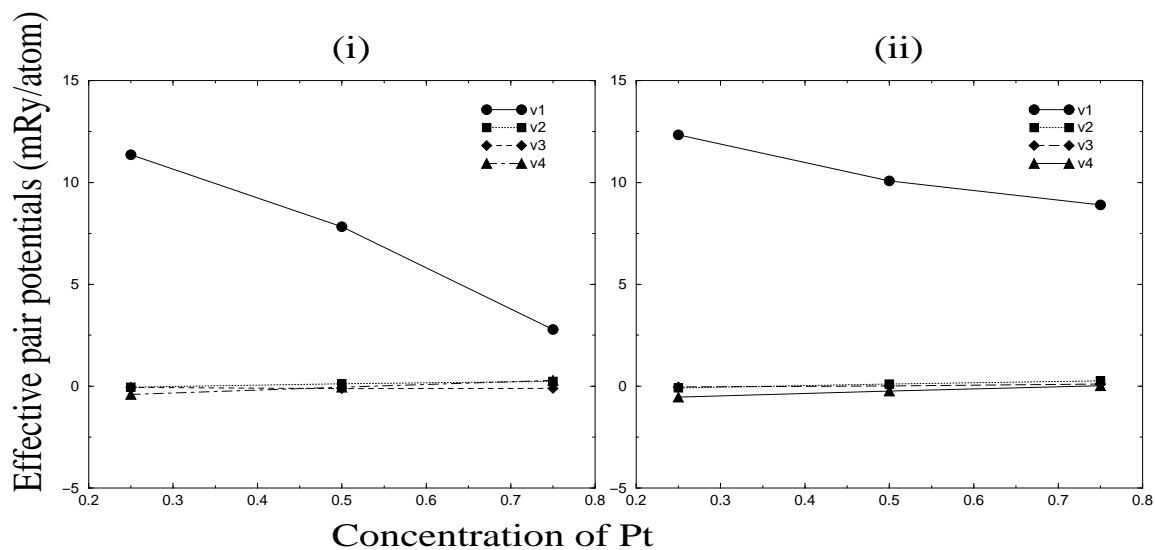


**Figure 5.** The effective pair potentials vs concentration of Pt with the choice of potential parameters with (i) charged spheres including scalar relativistic correction and (ii) charge neutral spheres including scalar relativistic correction.

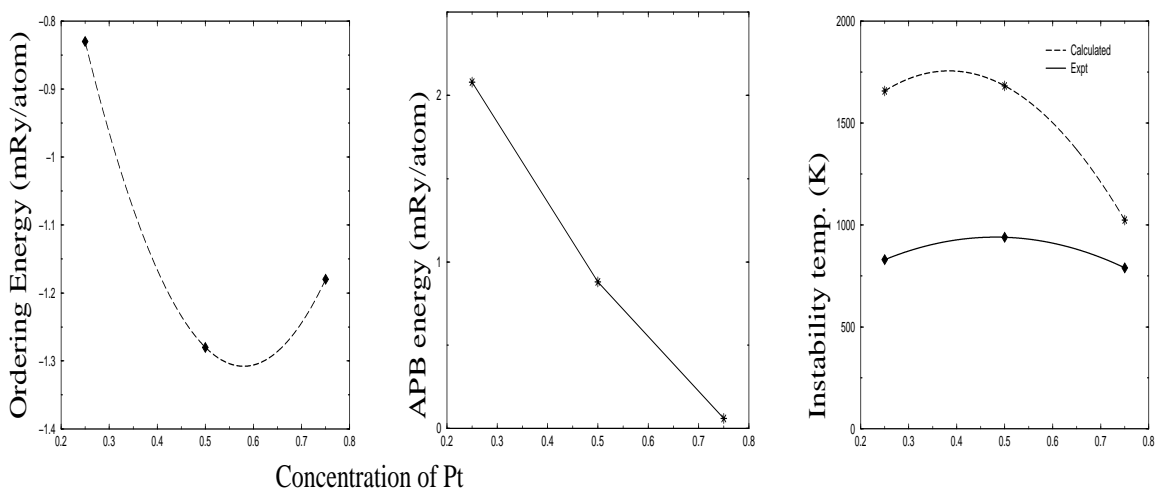


**Figure 6.** Ordering energy, anti-phase boundary energy and instability temperatures vs concentration of Pt with the choice of charge neutral potential parameters including scalar relativistic correction.